行政院國家科學委員會專題研究計畫 成果報告

雙亞硝醯基鐵化合物之合成，反應性研究及其電子結構與作為一氧化氮傳遞劑效率探討

研究成果報告(精簡版)

計 畫 類 別 ：個別型
計 畫 編 號 ：NSC 99-2119-M-040-001-
執 行 期 間 ：99 年 08 月 01 日至 100 年 07 月 31 日
執 行 單 位 ：中山醫學大學應用化學系（所）

計 畫 主 持 人：陳建宏

計畫參與人員：碩士級-專任助理人員：何怡潔
碩士級-專任助理人員：洪士軒
碩士班研究生-兼任助理人員：何怡潔
碩士班研究生-兼任助理人員：王正弘

處 理 方 式 ：本計畫涉及專利或其他智慧財產權，2 年後可公開查詢

中 華 民 國 100 年 08 月 25 日

New Members of the $\{Fe(NO)_2\}^{10}$ Dinitrosyl Iron Complexes (DNICs) Bound with [Thiolate, Thiolate] and [Amide, Amide] Ligations

Introduction

Interest in nitric oxide (NO) derives from its physiological and biological functions in living organisms.[1] In vivo, nitric oxide can be stabilized and stored in the two forms, protein-bound thionitrosyls ($R_{protein}$-SNO) and protein-bound dinitrosyl iron complexes (protein-bound DNICs).[2] The displacement of protein-bound DNICs with free thiols/thiolates yielding low-molecular-weight DNICs (LMW-DNICs) has been suggested.[3] In vitro/in vivo, both protein-bound DNICs and LMW DNICs are possibly identified and characterized by their distinctive electron paramagnetic resonance (EPR) signals at g = 2.03.[4] In spite of the major thiol components of cellular DNICs composed of cysteine and glutathione in vivo,[5] DNICs ligated by phenoxide, thiolate, imidazole, and deprotonated imidazole were proposed in enzymology based on EPR spectra.[3a,6] Recently, the protein-bound DNIC with [S,O] ligation has been well characterized by X-ray diffraction study via the addition of a dinitrosyldiglutathionyl iron complex into human glutathione transferase P1-1 in vitro/ in vivo.[6c] In biomimetic complexes, varieties of DNICs containing S/O/N-donor ligands were synthesized to serve as the spectroscopic references.[7,8] Based on the Enemark-Fetham notation,[9] these synthesized LMW DNICs can be classified as the EPR-active $\{Fe(NO)_2\}^9$ DNICs and the EPR-silent $\{Fe(NO)_2\}^{10}$ DNICs. In spite of a large number of the neutral $\{Fe(NO)_2\}^{10}$ DNICs with nitrogen or phosphorous liagnds, the dianionic $\{Fe(NO)_2\}^{10}$ DNICs are limited.[8] Recently, we report the monoanionic sulfur-containing $\{Fe(NO)_2\}^{10}$ DNIC [K-18-crown-6-ether][$Fe(SC_6H_4$-*o*-$NMe_2)(NO)_2$].[10] In addition to the classical four-coordinate DNICs, the non-classical DNICs, including the five-coordinate DNICs $[(6\text{-}Me_3\text{-TPA})Fe(NO)_2]^+$, [(TMEDA)$Fe(NO)_2$I],[11,12] and the six-coordinate DNIC [$(1\text{-Melm})_2(\eta^2\text{-ONO})Fe(NO)_2$],[13] are also structurally characterized. In this contribution, the dianionic $\{Fe(NO)_2\}^{10}$ DNICs with [thiolate,thiolate] and [amide,amide] ligation, $[Fe(SC_7H_4SN)_2(NO)_2]^{2-}$ (**1**) and $[Fe(OC_7H_4SN)_2(NO)_2]^{2-}$ (**2**) (cation = Na-18-crown-6-ether (**1-Na**/**2-Na**), PPh_4 (**1-PPh_4**/**2-PPh_4**)) were delineated. The reversible interconversion among the dianionic $\{Fe(NO)_2\}^{10}$ DNICs **1**/**2** and the anionic $\{Fe(NO)_2\}^9$ DNICs $[Fe(SC_7H_4SN)_2(NO)_2]^-$ (**3**)/$[Fe(OC_7H_4SN)_2(NO)_2]^-$ (**4**) (cation =

Na-18-crown-6-ether (**3-Na**/**4-Na**), PPh_4^+ (**3-PPh$_4$**/**4-PPh$_4$**)) were demonstrated. In particular, the different binding affinity of $[OC_7H_4SN]^-$ vs $[SC_7H_4SN]^-$ toward $\{Fe(NO)_2\}^9/\{Fe(NO)_2\}^{10}$ motif was studied.

Experimental Details

General Procedures. Manipulations, reactions, and transfers were conducted under nitrogen according to Schlenk techniques or in a glovebox (nitrogen gas). Solvents were distilled under nitrogen from appropriate drying agents (methylene chloride from CaH_2; acetonitrile from CaH_2-P_2O_5; diethyl ether, hexane and tetrahydrofuran(THF) from sodium benzophenone) and stored in dried, N_2-filled flasks over 4Å molecular sieves. Nitrogen was purged through these solvents before use. Solvent was transferred to the reaction vessel via stainless cannula under positive pressure of N_2. The reagents, iron pentacarbonyl (Strem), tetraphenylphosphonium bromide ([PPh_4][Br]), 18-crown-6-ether, nitrosonium tetrafluoroborate (Alfa Aesar), 2-mercaptobenzothiazole sodium salt, 2-hydroxybenzothiazole (TCI), ferrocenium hexafluorophosphate (Sigma-Aldrich) were used as received. $Fe(TMEDA)(NO)_2$ has been prepared according to the literature procedure.[1]

Physical Measurements. Infrared spectra of the nitrosyl ν(NO) stretching frequencies were recorded on Jasco FT/IR-4100 spectrophotometer/Bruker Alpha spectrophotometer with sealed solution cells (0.1 mm) and KBr windows. UV/vis spectra were recorded on a GBC Cintra 101. X-band EPR spectrum was recorded on a Bruker EMX spectrometer equipped with a Hewlett-Packard 5246 L electronic counter. Cyclic voltammetry (CV) was carried out with a CH Instruments electrochemical analyzer 611C. A three-electrode system consisted of a glassy carbon working electrode, a platinum wire auxiliary electrode, and a 0.1 M Ag/Ag^+ reference electrode. All CV data were recorded with the scan rate of 1 V s^{-1} in CH_3CN with tetrabutylammonium hexafluorophosphate as the supporting electrolyte. All potential values are reported verse ferrocene/ferrocenium ion. Analyses of carbon, hydrogen, and nitrogen were obtained with a CHN analyzer (Heraeus).

Crystallography. Crystallographic data and structure refinements parameters of complexes **1-PPh$_4$**, **2-PPh$_4$** and **4-PPh$_4$** are summarized in the Supplementary Material (Tables S1, S2 and S3). The crystals of complexes **1-PPh$_4$**, **2-PPh$_4$** and **4-PPh$_4$** chosen for X-ray diffraction studies are measured in size 0.38 x 0.25 x 0.07 mm, 0.58 × 0.40 × 0.32 mm, and 0.40 × 0.25 × 0.25 mm, respectively. Each crystal was mounted on a glass fiber and quickly coated in epoxy resin. Unit-cell parameters were obtained by least-squares refinement. Diffraction measurements for complexes **1-PPh$_4$**, **2-PPh$_4$** and **4-PPh$_4$** were carried out on a Nonius Kappa CCD and Bruker SMART Apex CCD diffractometers using graphite-monochromated Mo

K_α radiation (λ = 0.7107 Å) and between 2.22 and 25.06° for complex **1-PPh$_4$**, 2.26 and 25.04° for complex **2-PPh$_4$,** between 1.94 and 27.50° for complex **4-PPh$_4$**. Least-squares refinement of the positional and anisotropic thermal parameters for the contribution of all non-hydrogen atoms and fixed hydrogen atoms was based on F^2. A SADABS absorption correction was made. The SHELXTL structure refinement program was employed.

Preparation of [cation]$_2$[Fe(SC$_7$H$_4$SN)$_2$(NO)$_2$] (1) (cation = Na-18-crown-6-ether (1-Na), PPh$_4^+$ (1-PPh$_4$)). 1-Na: The compounds Fe(TMEDA)(NO)$_2$ (0.232 g, 1 mmol), [Na][SC$_7$H$_4$SN] (0.398 g, 2 mmol) and 18-crown-6-ether (0.528 g, 2 mmol) were loaded into a Schlenk tube, and then 20 mL of THF was added under positive N_2 at ambient temperature. The reaction solution was stirred overnight and then the light green precipitates were afforded. When the upper solution was discarded via cannula under a positive pressure of N_2, the residual light green solid was washed with 15 mL of THF. After drying the light green solid under vacuum, the light green solid of [Na-18-crown-6-ether]$_2$[Fe(SC$_7$H$_4$SN)$_2$(NO)$_2$] (**1-Na**) (yield: 0.95 g, 92.9 %) was afforded. IR: 1684 (s)，1633 (s) cm^{-1} (CH_3CN); 1654 (s), 1609 (s) (ν_{NO}) cm^{-1} (KBr). Absorption spectrum (THF) [λ_{max}, nm (ε, M^{-1} cm^{-1})]: 670 (307), 488 (781). **1-PPh$_4$**: To the CH_3CN solution (10 mL) of (TMEDA)Fe(NO)$_2$ (0.232 g, 1 mmol) was added the CH_3CN solution (20 mL) of [PPh$_4$][SC$_7$H$_4$SN] (1.012 g, 2 mmol) dropwise under N_2 at ambient temperature. After storing the reaction solution without stirring for 5 days under nitrogen atmosphere at -15°C, the upper solution was discarded by cannula under positive N_2 pressure and then the brown crystals suitable for single-crystal X-ray diffraction was dried under vacuum to afford [PPh$_4$]$_2$[Fe(SC$_7$H$_4$SN)$_2$(NO)$_2$] (**1-PPh$_4$**) (yield: 0.878 g, 77.9%). IR: 1661 (s), 1613 (s) cm^{-1} (ν_{NO}) (KBr). Anal. Calcd for $C_{62}H_{48}FeN_4O_2P_2S_4$: C, 66.07; H, 4.29; N, 4.97. Found: C, 66.51; H, 3.88; O, 4.63.

Preparation of [cation]$_2$[Fe(OC$_7$H$_4$SN)$_2$(NO)$_2$] (2) (cation = Na-18-crown-6-ether (2-Na), PPh$_4$ (2-PPh$_4$)). 2-Na: The compounds Fe(TMEDA)(NO)$_2$ (0.232 g, 1 mmol), [Na][OC$_7$H$_4$SN] (0.346 g, 2 mmol) and 18-crown-6-ether (0.528 g, 2 mmol) were loaded into a Schlenk flask, and then 10 mL of THF was added under positive N_2 at ambient temperature. The reaction solution was stirred overnight and then 40 mL of diethyl ether was added to the reaction solution. After the reaction mixture was stirred for 1 h, the light green precipitates were afforded. The upper solution was discarded via cannula under a positive pressure of N_2 and the residual light green solid was washed with 20 mL of diethyl ether. After drying the light green solid under vacuum, the light green solid of [Na-18-crown-6-ether]$_2$[Fe(OC$_7$H$_4$SN)$_2$(NO)$_2$] (**2-Na**) (yield: 0.65 g, 65.7%) was

afforded. IR: 1665 (m)，1609 (sh) (ν_{NO}), 1627 (s) (ν_{CO}) cm^{-1} (CH_3CN); 1664 (s), 1606 (s) (ν_{NO}), 1623 (s) (ν_{CO}) cm^{-1} (KBr). Absorption spectrum (THF) [λ_{max}, nm (ε, M^{-1} cm^{-1})]: 712 (125), 390 (858). **2-PPh$_4$**: To the CH_3CN solution (10 mL) of (TMEDA)$Fe(NO)_2$ (0.162 g, 0.7 mmol) was added the CH_3CN solution (20 mL) of $[PPh_4][OC_7H_4SN]$ (0.685 g, 1.4 mmol) dropwise under N_2 at ambient temperature. After storing the reaction solution without stirring for 5 days under nitrogen atmosphere at -15°C, the upper solution was discarded by cannula under positive N_2 pressure and then the brown crystals suitable for single-crystal X-ray diffraction was dried under vacuum to afford $[PPh_4]_2[Fe(OC_7H_4SN)_2(NO)_2]$ (**2-PPh$_4$**) (yield: 0.457 g, 59.6 %). IR: 1662 (s), 1637 (s) (ν_{NO}) cm^{-1} (KBr). Anal. Calcd for $C_{62}H_{48}FeN_4O_4P_2S_2$: C, 68.01; H, 4.42; N, 5.12. Found: C, 67.73; H, 4.05; N, 5.50.

Reaction of [cation]$_2$[Fe(SC$_7$H$_4$SN)$_2$(NO)$_2$] (1) with [Cp$_2$Fe][PF$_6$] (cation = Na-18-crown-6-ether (1-Na), PPh$_4^+$ (1-PPh$_4$)). 1-Na: The 10 mL CH_3CN solution of $[Cp_2Fe][PF_6]$ (0.497 g, 1.5 mmol) was added dropwise into the 50 mL Schlenk flask containing CH_3CN solution of complex **1-Na** (1.534 g, 1.5 mmol) via a cannula under positive N_2 pressure at 0℃. After being stirred for 5 h, the reaction solution was dried under vacuum to afford the brown solid. 30 mL of THF was added to dissolve the brown solid and the resulting THF solution was monitored with FTIR. The IR spectrum showing ν_{NO} stretching frequencies at 1767 (s), 1716(s) cm^{-1} (THF) was assigned to the formation of [Na-18-crown-6-ether][Fe(SC$_7$H$_4$SN)$_2$(NO)$_2$] (**3-Na**).[2] The THF solution was filtered through Celite to separate insoluble [Na-18-crown-6-ether][PF_6]. The brown filtrate was concentrated to 5 mL and 40 mL hexane was added to precipitate the brown solid. The brown solid was washed with 20 mL of diethyl ether twice and dried under vacuum to yield complex **3-Na** (yield: 1.03 g, 93.6 %). IR: 1773 (s), 1721 (s) (ν_{NO}) cm^{-1} (CH_3CN); 1768 (s), 1729 (s) (ν_{NO}) cm^{-1} (KBr). Absorption spectrum (THF) [λ_{max}, nm (ε, M^{-1} cm^{-1})]: 788 (491), 457 (2918). **1-PPh$_4$**: The 5 mL CH_3CN solution of $[Cp_2Fe][PF_6]$ (0.099 g, 0.3 mmol) was added dropwise into the 50 mL Schlenk flask containing CH_3CN solution of complex **1-PPh$_4$** (0.338 g, 0.3 mmol) via a cannula under positive N_2 pressure at 0℃. After being stirred for 5 h, the reaction solution was dried under vacuum to afford the brown solid. 10 mL of THF was added to dissolve the brown solid and the resulting THF solution was monitored with FTIR. The IR spectrum showing ν_{NO} stretching frequencies at 1767 (s), 1716(s) cm^{-1} (THF) was assigned to the formation of $[PPh_4][Fe(SC_7H_4SN)_2(NO)_2]$ (**3-PPh$_4$**).[3] The THF solution was filtered through Celite to separate insoluble $[PPh_4][PF_6]$. The brown filtrate was concentrated to 5 mL and 25 mL diethyl ether was added to precipitate the brown solid. The brown solid was washed with 20 mL of diethyl ether twice and dried under vacuum to yield

complex **3-PPh$_4$** (yield: 0.182 g, 76.7 %). IR: 1774 (s), 1721 (s) (ν_{NO}) cm^{-1} (CH_3CN); 1781 (s), 1739 (s) (ν_{NO}) cm^{-1} (KBr).

Reaction of [cation]$_2$[Fe(OC$_7$H$_4$SN)$_2$(NO)$_2$] (2) with [Cp$_2$Fe][PF$_6$] (cation = Na-18-crown-6-ether (2-Na), PPh$_4^+$ (2-PPh$_4$)). 2-Na: The 8 mL CH_3CN solution of [Cp_2Fe][PF_6] (0.331 g, 1 mmol) was added dropwise into the 50 mL Schlenk flask containing CH_3CN solution of complex **2-Na** ((0.991 g, 1 mmol) via a cannula under positive N_2 pressure at 0℃. After being stirred for 5 h, the reaction solution was dried under vacuum to afford the brown solid. 20 mL of THF was added to dissolve the brown solid and the resulting THF solution was monitored with FTIR. The IR spectrum showing ν_{NO} stretching frequencies at 1786 (m), 1714(s) cm^{-1} (THF) was assigned to the formation of [Na-18-crown-6-ether][Fe(OC_7H_4SN)$_2$(NO)$_2$] (**4-Na**). The THF solution was filtered through Celite to separate insoluble [Na-18-crown-6-ether][PF_6]. The brown filtrate was concentrated to 5 mL and 40 mL diethyl ether was added to precipitate the brown solid. The brown solid was washed with 20 mL of diethyl ether twice and dried under vacuum to yield complex **4-Na** (yield 0.585 g, 83.1 %). IR: 1791 (m), 1723 (s) (ν_{NO}), 1634 (s) (ν_{CO}) cm^{-1} (CH_3CN); 1786 (s), 1696 (s) (ν_{NO}), 1626 (s) (ν_{CO}) cm^{-1} (KBr). Absorption spectrum (THF) [λ_{max}, nm (ε, M^{-1} cm^{-1})]: Absorption spectrum (THF) [λ_{max}, nm (ε, M^{-1} cm^{-1})]: 721 (281), 440 (1719). **2-PPh$_4$**: The 5 mL CH_3CN solution of [Cp_2Fe][PF_6] (0.099 g, 0.3 mmol) was added dropwise into the 50 mL Schlenk flask containing CH_3CN solution of complex **2-PPh$_4$** (0.329 g, 0.3 mmol) via a cannula under positive N_2 pressure at 0℃. After being stirred for 5 h, the reaction solution was dried under vacuum to afford the brown solid. 10 mL of THF was added to dissolve the brown solid and the resulting THF solution was monitored with FTIR. The IR spectrum showing ν_{NO} stretching frequencies at 1786 (m), 1718(s) cm^{-1} (THF) was assigned to the formation of [PPh_4][Fe(OC_7H_4SN)$_2$(NO)$_2$] (**4-PPh$_4$**). The THF solution was filtered through Celite to separate insoluble [PPh_4][PF_6]. The brown filtrate was concentrated to 5 mL and 25 mL diethyl ether was added to precipitate the red-brown solid. The red-brown solid was washed with 20 mL of diethyl ether twice and dried under vacuum to yield complex **4-PPh$_4$** (yield: 0.141 g, 61.9 %). Diffusion of diethyl ether into the THF solution of complex **4-PPh$_4$** at -15 ℃ led to red-brown crystals suitable for single-crystal X-ray diffraction. IR: 1791 (m), 1723 (s) (ν_{NO}), 1636 (m) (ν_{CO}) cm^{-1} (CH_3CN); 1785 (s), 1718 (s) (ν_{NO}), 1636 (m), 1623 (s) (ν_{CO}) cm^{-1} (KBr). EPR (THF) at 298 K: g = 2.031. Anal. Calcd for $C_{38}H_{28}FeN_4O_4PS_2$: C, 60.40; H, 3.74; N, 7.41. Found: C, 60.71; H, 3.54; N, 7.72.

Reaction of complex 3-PPh$_4$ with [PPh$_4$][OC$_7$H$_4$SN]. The compounds, complex **3-PPh$_4$** (0.157 g, 0.2 mmol) and [PPh_4][OC_7H_4SN] (0.197 g, 0.4 mmol)

were loaded into a Schlenk tube, and then 10 mL of THF was added under positive N_2 at ambient temperature. After being stirred overnight, the solution was monitored with FTIR. The IR spectrum showing ν_{NO} stretching frequencies at 1786 (m), 1718(s) cm^{-1} (THF) was assigned to the formation of complex **4-PPh$_4$**. The THF solution was filtered through Celite to separate insoluble $[PPh_4][SC_7H_4SN]$. The brown filtrate was concentrated to 5 mL and 25 mL diethyl ether was added to precipitate the brown solid. The brown solid was washed with 20 mL of diethyl ether twice and dried under vacuum to yield complex **4-PPh$_4$** (yield: 0.134 g, 88.7 %).

Reaction of complex 2-Na with [Na][SC$_7$H$_4$SN] and 18-crown-6-ether. The compounds, complex **2-Na** (0.495 g, 0.5 mmol), $[Na][SC_7H_4SN]$ (0.189 g, 1 mmol) and 18-crown-6-ether (0.264 g, 1 mmol) were loaded into a Schlenk flask, and then 10 mL of THF was added under positive N_2 at ambient temperature. After being stirred overnight, the light green precipitates were afforded. When the upper solution was discarded via cannula under a positive pressure of N_2, the residual light green solid was washed with 10 mL of THF. After drying the light green solid under vacuum and identifying by FTIR (IR: 1654 (s), 1609 (s) cm^{-1} (ν_{NO}) (KBr)), the light green solid of $[Na\text{-}18\text{-}crown\text{-}6\text{-}ether]_2[Fe(SC_7H_4SN)_2(NO)_2]$ (**1-Na**) (yield: 0.44 g, 86.3 %) was afforded.

Reaction of complex 3-PPh$_4$ with CoCp$_2$ (or Reaction of 4-PPh$_4$ with CoCp$_2$). Complex **3-PPh$_4$** (0.236 g, 0.3 mmol) (or complex **4-PPh$_4$** (0.227 g, 0.3 mmol))and $CoCp_2$ (0.057 g, 0.3 mmol) were dissolved in THF (8 mL) and stirred overnight under nitrogen at ambient temperature. After being stirred overnight, the upper solution was discarded via cannula under a positive pressure of N_2, and the residual light green solids (or light brown solids) were washed with 15 mL of diethyl ether. The IR spectrum of the light brown solids showed the ν_{NO} stretching frequencies at 1652 (s), 1602(s) cm^{-1} (KBr) was assigned to the formation of $[PPh_4][CoCp_2]$ $[Fe(SC_7H_4SN)_2(NO)_2]$ (The IR spectrum of the light green solids showed the ν_{NO} stretching frequencies at 1663 (s), 1636(s) cm^{-1} (KBr) was assigned to the formation of $[PPh_4][CoCp_2]$ $[Fe(OC_7H_4SN)_2(NO)_2]$. After drying the light green solids under vacuum, light green solids of $[PPh_4][CoCp_2]$ $[Fe(SC_7H_4SN)_2(NO)_2]$ (yield: 0.18 g, 61.4 %) (or brown solid of $[PPh_4][CoCp_2]$ $[Fe(OC_7H_4SN)_2(NO)_2]$ (yield: 0.23 g, 81.2 %)) were afforded.

Reaction of complex 3-PPh$_4$ with complex 2-PPh$_4$. Complex **3-PPh$_4$** (0.157 g, 0.2 mmol) and complex **2-PPh$_4$** (0.218 g, 0.2 mmol) were loaded into a Schlenk flask, and then 6 mL of THF and 2 mL of CH_3CN were added under positive N_2 at ambient temperature. After being stirred for 3 days, 15 mL of hexane was added to the reaction mixture. When the reaction mixture was stand for several minutes, the upper red solution was transferred to the other flask via cannula under a positive

pressure of N_2. The residual solid was washed with 10 mL of THF and the THF solution was transferred to the above flask via cannula under a positive pressure of N_2. After drying the light green solid under vacuum and identifying by FTIR (IR: 1661 (s), 1613 (s) cm^{-1} (ν_{NO}) (KBr)), the light green solid of complex **1-PPh$_4$** (yield: 0.158 g, 70.2 %) was afforded. In addition, the solution of the other flask was concentrated to 5 mL and 35 mL diethyl diether was added to precipitate the red solid. The IR spectrum of the red solids showed the ν_{NO} stretching frequencies at 1785 (s), 1718(s) cm^{-1} (KBr) was assigned to the formation of complex **4-PPh$_4$** and the yield was 92.7 % (0.140 g).

Results and Discussion

Reaction of $Fe(TMEDA)(NO)_2$ with 2 equiv of $[SC_7H_4SN]^-$ and $[OC_7H_4SN]^-$ yielded DNICs **1** and **2** characterized by single-crystal X-ray diffraction, IR and UV/vis spectra, respectively (Scheme 1a and 1b). DNICs **1** and **2** display the EPR-silent $\{Fe(NO)_2\}^{10}$ electronic structures with [thiolate, thiolate]/[amide, amide] ligation mode. Compared to the other $\{Fe(NO)_2\}^{10}$ DNICs, **1-PPh$_4$** is the first example of the dianionic mononuclear $\{Fe(NO)_2\}^{10}$ DNICs coordinated with two thiolate ligands.

Upon the addition of Cp_2FePF_6 into the CH_3CN solution of DNICs **1** and **2** in a 1:1 stoichiometry, respectively (Scheme 1c and 1d), oxidation ensued over the course of 5 h to yield the $\{Fe(NO)_2\}^9$ DNICs **3** and **4**, respectively, identified by EPR and IR spectra. In contrast to the ligand-centered oxidation of the thiolate-containing $\{Fe(NO)_2\}^9$ DNICs resulting in dimeric $\{Fe(NO)_2\}^9$-$\{Fe(NO)_2\}^9$ RREs,[7c,7f] the isolation of DNIC **3** may reveal that the oxidation of thiolate-containing $\{Fe(NO)_2\}^{10}$ DNICs is a metal-centered process.

In cyclic voltammograms of **3-PPh$_4$** and **4-PPh$_4$**, the quasi-reversible one-electron reduction at -0.94 and -1.17 V ($E_{1/2}$ vs Fc^+/Fc), respectively, in CH_3CN are observed and assigned to the $\{Fe(NO)_2\}^9$-$\{Fe(NO)_2\}^{10}$ couple (Figure S1 in the Supporting Information). The slightly negative reduction potential of **4-PPh$_4$** than that of **3-PPh$_4$** indicates that $[OC_7H_4SN]^-$ performs the stronger electron-donating ability than $[SC_7H_4SN]^-$. Chemical reduction of **3-PPh$_4$** and **4-PPh$_4$** with $CoCp_2$ (Scheme 1c' and 1d') afforded $\{[PPh_4][CoCp_2]\}\{[Fe(SC_7H_4SN)_2(NO)_2]\}$ and $\{[PPh_4][CoCp_2]\}\{[Fe(OC_7H_4SN)_2(NO)_2]\}$, respectively, characterized by FTIR. The reduction process is also consistent with the $\{Fe(NO)_2\}^9$-$\{Fe(NO)_2\}^{10}$ couple in the cyclic voltammogram of **3-PPh$_4$**/**4-PPh$_4$**. In contrast to the reduction of the thiolate-containing $\{Fe(NO)_2\}^9$ DNICs leading to the dissociation of thiolate of DNICs reported previously,[7b] the redox reaction of DNICs **3** and **1** displays the

reversible interconversion between the thiolate-containing $\{Fe(NO)_2\}^9$ and $\{Fe(NO)_2\}^{10}$ DNICs.

Scheme 1.

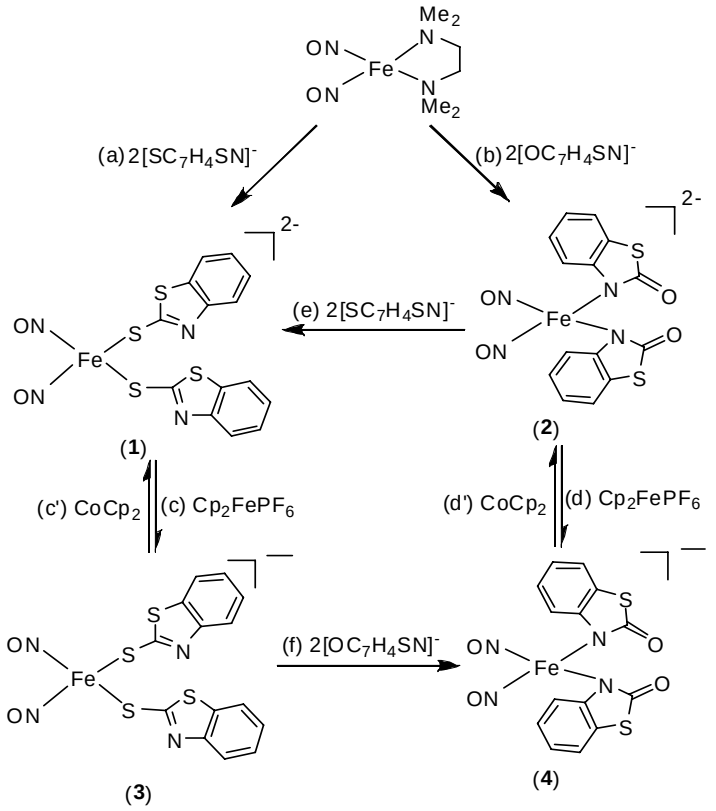

1-Na, **2-Na**, **3-Na**, **4-Na** : cation = Na-18-crown-6-ether

1-PPh$_4$, **2-PPh$_4$**, **3-PPh$_4$**, **4-PPh$_4$** : cation = PPh_4

The relative affinity of the different ligands toward the $\{Fe(NO)_2\}^9$ motif has been studied by Liaw et al. via the ligand-exchange experiments.[7b,7g,7j] Similarly, the coordinated ligands $[SC_7H_4SN]^-$ of $\{Fe(NO)_2\}^9$ **3-PPh$_4$** could be replaced by the stronger donor $[OC_7H_4SN]^-$ to yield the more stable **4-PPh$_4$** (Scheme 1f). Interestingly, the addition of 2 equiv of $[SC_7H_4SN]^-$ to the THF solution of $\{Fe(NO)_2\}^{10}$ **2-Na** led to the light green precipitates of the more stable **1-Na**, characterized by IR spectra (Scheme 1e). The different binding affinity of $[OC_7H_4SN]^-$ and $[SC_7H_4SN]^-$ toward the $\{Fe(NO)_2\}$ core of DNICs reveals that the electron-rich $\{Fe(NO)_2\}^{10}$ motif prefers the binding of the less electron-donating ligand $[SC_7H_4SN]^-$. In contrast, the stronger electron-donating ligand $[OC_7H_4SN]^-$ favors to coordinate to the electron-deficient $\{Fe(NO)_2\}^9$ motif. This rationalization may support that reaction of $\{Fe(NO)_2\}^{10}$ **2-PPh$_4$** and $\{Fe(NO)_2\}^9$ **3-PPh$_4$** afforded the relatively stable $\{Fe(NO)_2\}^9$ **4-PPh$_4$** and $\{Fe(NO)_2\}^{10}$ **1-PPh$_4$** via intermolecular electron transfer in THF (Scheme 2).

Scheme 2.

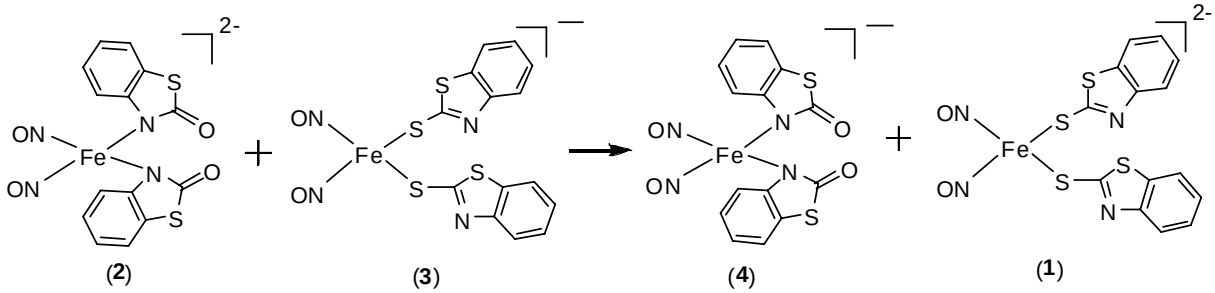

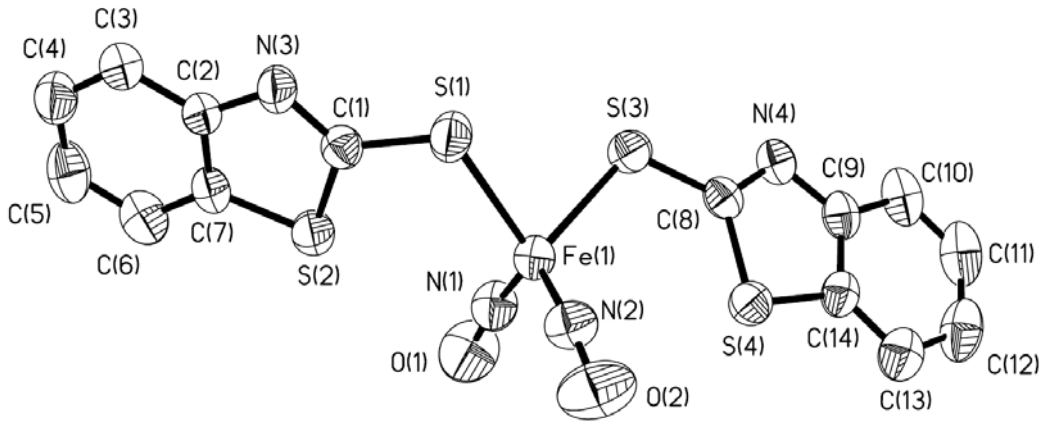

Figure 1. Structure of anion of **1-PPh$_4$** displaying 50% thermal ellipsoids for all non-hydrogen atoms. Selected bond distances (Å) and angles (deg): Fe(1)−N(1), 1.645(4); Fe(1)−N(2), 1.642(4); Fe(1)−S(1), 2.3679(13); Fe(1)−S(3), 2.3240(13); N(1)−O(1), 1.193(4); N(2)−O(2), 1.205(4); Fe(1)−N(1)−O(1), 168.3(4); Fe(1)−N(2)−O(2), 167.6(4); N(1)−Fe(1)−N(2), 115.34(19); S(1)−Fe(1)−S(3), 84.48(5).

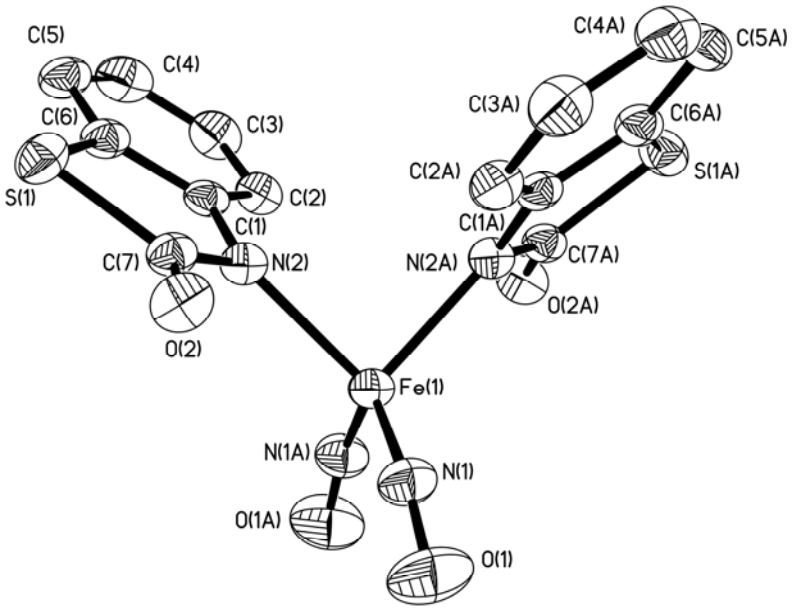

Figure 2. Structure of anion of **2-PPh$_4$** displaying 50% thermal ellipsoids for all non-hydrogen atoms. Selected bond distances (Å) and angles (deg): Fe(1)−N(1), 1.638(3); Fe(1)−N(2), 2.094(2); N(1)−O(1), 1.203(3); N(1)−Fe(1)−N(1A), 110.45(19); N(2)−Fe(1)−N(2A), 88.80(13); Fe(1)−N(1)−O(1), 164.6(3).

Figures 1 and 2 display the thermal ellipsoid plots of the dianionic **1-PPh$_4$** and **2-PPh$_4$**, respectively, and the selected bond angles and bond lengths are given in the figure captions, respectively. The structures of **1-PPh$_4$** and **2-PPh$_4$** contain a four-coordinate iron center in a distorted tetrahedral geometry. The comparisons of mean Fe-S bond distances (2.2941(18) Å in [PPN][Fe(SC$_7$H$_4$SN)$_2$(NO)$_2$][7b] vs 2.3460(13) Å in **1-PPh$_4$**) and Fe-N bond distances (1.993(2) Å in **4-PPh$_4$** (Figure S2 in the Supporting Information) vs 2.094(2) Å in **2-PPh$_4$**) reveal that reduction of {Fe(NO)$_2$}^{9} core to {Fe(NO)$_2$}^{10} core lead to the elongation of Fe−N and Fe−S distances. Meanwhile, the shorter Fe−N(O) bond distances of 1.644(4) Å and 1.638(3) Å and the longer N−O bond distances of 1.199(4) Å and 1.203(3) Å found in **1-PPh$_4$** and **2-PPh$_4$**, respectively, compared to the Fe−N(O) bond distances of 1.684(6) Å and 1.687(2) Å and the N−O bond distances of 1.174(6) Å and 1.175(3) found in [PPN][Fe(SC$_7$H$_4$SN)$_2$(NO)$_2$] and **4-PPh$_4$**, respectively, are consistent with a relatively considerable degree of π-backbonding in the {Fe(NO)$_2$}^{10} core. In contrast to the distinct bond distances in [PPN][Fe(SC$_7$H$_4$SN)$_2$(NO)$_2$] and **1-PPh$_4$**/**4-PPh$_4$** and **2-PPh$_4$**, the comparable Fe−N−O bond angles (169.9(5)° in [PPN][Fe(SC$_7$H$_4$SN)$_2$(NO)$_2$] vs 168.0(4)° in **1-PPh$_4$** and 163.6(2) ° in **4-PPh$_4$** vs 164.6(3) ° in **2-PPh$_4$**) are observed when the {Fe(NO)$_2$}^{9} DNICs are reduced to the structurally analogous {Fe(NO)$_2$}^{10} DNICs.

In summary, the dianionic $\{Fe(NO)_2\}^{10}$ DNICs containing [thiolate,thiolate]/[amide/amide] ligation were isolated and structurally characterized. The synthetic methodology reveals that $Fe(TMEDA)(NO)_2$ acts as an $\{Fe(NO)_2\}^{10}$ motif-donor reagent in the presence of thiolates and amides. Redox reaction between DNICs **1**/**2** and DNICs **3**/**4** successfully demonstrate the reversible interconversion with no dissociation of the coordinated ligands of the structurally analogous $\{Fe(NO)_2\}^9$/$\{Fe(NO)_2\}^{10}$ DNICs. The ligand substitution reactions of DNICs **2** and **3** to form the relatively stable DNICs **1** and **4**, respectively, have demonstrated that the $\{Fe(NO)_2\}^9$ motif shows strong preference for the stronger electron-donating ligands over the weaker electron-donating ligands; however, the $\{Fe(NO)_2\}^{10}$ motif shows the stronger binding affinity toward the weaker electron-donating ligands. In addition to the ligand-exchange reactions yielding the more stable DNICs,[7b,7g,7j] the reaction of $\{Fe(NO)_2\}^{10}$ **2-PPh$_4$** and $\{Fe(NO)_2\}^9$ **3-PPh$_4$** yielding the relatively stable $\{Fe(NO)_2\}^9$ **4-PPh$_4$** and $\{Fe(NO)_2\}^{10}$ **1-PPh$_4$** may signify that the intermolecular electron transfer between $\{Fe(NO)_2\}^{10}$ and $\{Fe(NO)_2\}^9$ DNICs is the alternative mechanism to afford the more stable DNICs for transport and storage of NO in biology. Studies on the electronic structure (NO/Fe oxidation states) of the series of $\{Fe(NO)_2\}^9$/$\{Fe(NO)_2\}^{10}$ DNICs by X-ray absorption spectroscopy and DFT calculations are ongoing. Also, the binding preference of a series of ligands toward $\{Fe(NO)_2\}^9$/$\{Fe(NO)_2\}^{10}$ motifs are currently being investigated in our laboratory.

Reference

(1)(a) Jaimes, E. A.; del Castillo, D.; Rutherford, M. S.; Raij, L., *J. Am. Soc. Nephrol.* **2001,** *12*, 1204-1210. (b) May, G. C., P.; Moore, PK.; Page, CP., *Br. J. Pharmacol* **1991,** *102*, 759-763. (c) Tao, Y. P.; Misko, T. P.; Howlette, A. C.; Klein, C., *Development* **1997,** *124*, 3587-3595. (d) MacMicking, J.; Xie, Q.; Nathan, C., *Annu. Rev. Immuno.* **1997,** *15*, 323-350.

(2)(a) McCleverty, J. A., *Chem. Rev.* **2004,** *104*, 403-418. (b) Badorff, C.; Fichtlscherer, B.; Muelsch, A.; Zeiher, A. M.; Dimmeler, S., *Nitric Oxide* **2002,** *6*, 305-312. (c) Stamler, J. S.; Singel, D. J.; Loscalzo, J., *Science* **1992,** *258*, 1898-1902. (d) Stamler, J. S., *Cell* **1994,** *78*, 931-936.

(3)(a) Boese, M.; Mordvintcev, P. I.; Vanin, A. F.; Busse, R.; Muelsch, A., *J. Biol. Chem.* **1995,** *270*, 29244-29249. (b) Henry, Y.; Lepoivre, M.; Drapier, J. C.; Ducrocq, C.; Boucher, J. L.; Guissani, A., *FASEB J.* **1993,** *7*, 1124-1134. (c) Radi, R.; Beckman, J. S.; Bush, K. M.; Freeman, B. A., *J. Biol. Chem.* **1991,** *266*, 4244-4250. (d) Mulsch, A., *Drug Res.* **1994,** *44*, 408-411. (e) Vanin, A. F.; Mordvintcev, P. I.; Hauschildt, S.; Muelsch, A., *Biochim. Biophys. Acta, Mol.*

Cell Res. **1993,** *1177*, 37-42.

(4)(a) Butler, A. R.; Megson, I. L., *Chem. Rev.* **2002,** *102*, 1155-1165. (b) Cooper, C. E., *Biochim. Biophys. Acta, Bioenergy* **1999,** *1411*, 290-309. (c) Foster, M. W.; Cowan, J. A., *J. Am. Chem. Soc.* **1999,** *121*, 4093-4100. (d) Vithayathil, A. J.; Ternberg, J. L.; Commoner, B., *Nature* **1965,** *207*, 1246-1249.

(5)Lewandowska, H.; Meczynska, S.; Sochanowicz, B.; Sadlo, J.; Kruszewski, M., *J. Biol. Inorg. Chem.* **2007,** *12*, 345-352.

(6)(a) Ding, H.; Demple, B., *Proc. Natl. Acad. Sci. U. S. A.* **2000,** *97*, 5146-5150. (b) Turella, P.; Pedersen, J. Z.; Caccuri, A. M.; De Maria, F.; Mastroberardino, P.; Lo Bello, M.; Federici, G.; Ricci, G., *J. Biol. Chem.* **2003,** *278*, 42294-42299. (c) Cesareo, E.; Parker, L. J.; Pedersen, J. Z.; Nuccetelli, M.; Mazzetti, A. P.; Pastore, A.; Federici, G.; Caccuri, A. M.; Ricci, G.; Adams, J. J.; Parker, M. W.; Lo Bello, M., *J. Biol. Chem.* **2005,** *280*, 42172-42180. (e) D'Autreaux, B.; Horner, O.; Oddou, J.-L.; Jeandey, C.; Gambarelli, S.; Berthomieu, C.; Latour, J.-M.; Michaud-Soret, I., *J. Am. Chem. Soc.* **2004,** *126*, 6005-6016.

(7) (a) Tsai, M.-L.; Chen, C.-C.; Hsu, I. J.; Ke, S.-C.; Hsieh, C.-H.; Chiang, K.-A.; Lee, G.-H.; Wang, Y.; Chen, J.-M.; Lee, J.-F.; Liaw, W.-F., *Inorg. Chem.* **2004,** *43*, 5159-5167. (b) Tsai, F. T.; Chiou, S. J.; Tsai, M. C.; Tsai, M. L.; Huang, H. W.; Chiang, M. H.; Liaw, W. F., *Inorg. Chem.* **2005,** *44*, 5872-5881. (c) Lu, T.-T.; Chiou, S.-J.; Chen, C.-Y.; Liaw, W.-F., *Inorg. Chem.* **2006,** *45*, 8799-8806. (d) Tsai, M.-L.; Liaw, W.-F., *Inorg. Chem.* **2006,** *45*, 6583-6585. (e) Hung, M.-C.; Tsai, M.-C.; Lee, G.-H.; Liaw, W.-F., *Inorg. Chem.* **2006,** *45*, 6041-6047. (f) Tsai, M. L.; Hsieh, C. H.; Liaw, W. F., *Inorg. Chem.* **2007,** *46*, 5110-5117. (g) Huang, H.-W.; Tsou, C.-C.; Kuo, T.-S.; Liaw, W.-F., *Inorg. Chem.* **2008,** *47*, 2196-2204. (h) Chiou, S.-J.; Wang, C.-C.; Chang, C.-M., *J. Organomet. Chem.* **2008,** *693*, 3582-3586. (i) Wang, X.; Sundberg, E. B.; Li, L.; Kantardjieff, K. A.; Herron, S. R.; Lim, M.; Ford, P. C., *Chem. Commun.* **2005**, 477-479. (j) Tsai, M.-C.; Tsai, F.-T.; Lu, T.-T.; T, M.-L.; Wei, Y.-C.; Hsu, I.-J.; Lee, J.-F.; Liaw, W.-F. *Inorg. Chem.* **2009,** *48*, 9579-9591.

(8)(a) Reginato, N.; McCrory, C. T. C.; Pervitsky, D.; Li, L., *J. Am. Chem. Soc.* **1999,** *121*, 10217-10218. (b) Wang, R.; Wang, X.; Sundberg, E. B.; Nguyen, P.; Grant, G. P.; Sheth, C.; Zhao, Q.; Herron, S.; Kantardjieff, K. A.; Li, L., *Inorg. Chem.* **2009,** *48*, 9779-9785. (c) Albano, V. G.; Araneo, A.; Bellon, P. L.; Ciani, G.; Manassero, M., *J. Organomet. Chem.* **1974,** *67*, 413-422. (d) Atkinson, F. L.; Blackwell, H. E.; Brown, N. C.; Connelly, N. G.; Crossley, J. G.; Orpen, A. G.; Rieger, A. L.; Rieger, P. H., *Dalton Trans* **1996**, 3491-3502. (e) Tonzetich, Z. J.; Do, L. H.; Lippard, S. J., *J. Am. Chem. Soc.* **2009,** *131*, 7964-7965.

(9)Enemark, J. H.; Feltham, R. D., *Coord. Chem. Rev.* **1974,** *13*, 339-406.

(10) Chen, C. H.; Chiou, S. J.; Chen, H. Y., *Inorg. Chem.* **2010,** *49*, 2023-2025.
(11) Jo, D.-H.; Chiou, Y.-M.; Que, L., Jr., *Inorg. Chem.* **2001,** *40*, 3181-3190.
(12) Chen, C.-H.; Ho, Y.-C.; Lee, G.-H., *J. Organomet. Chem.* **2009,** *694*, 3395-3400.
(13) Tsai, F. T.; Kuo, T. S.; Liaw, W. F., *J. Am. Chem. Soc.* **2009,** *131*, 3426-3427.

Supplementary Material

Contents:

Figures

Tables

Figures

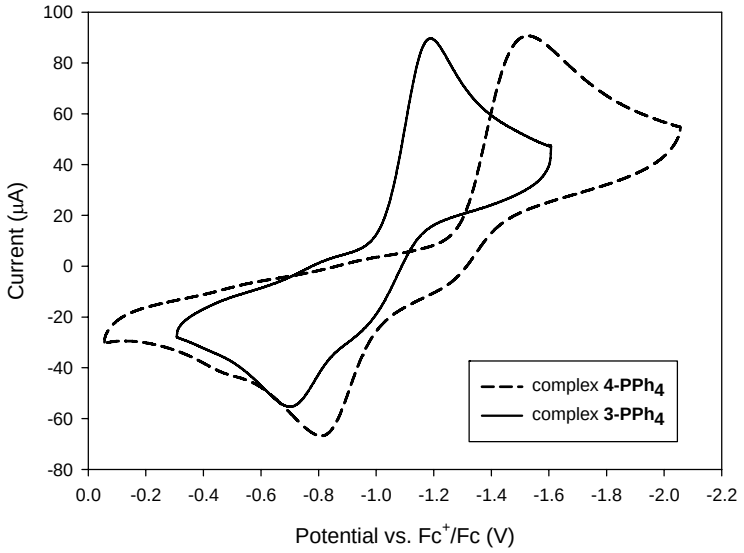

Figure S1. Cyclic voltammograms of 2.5 mM CH_3CN solution of $[PPh_4][Fe(SC_7H_4SN)_2(NO)_2]$ (**3-PPh$_4$**) (solid line) and $[PPh_4][Fe(OC_7H_4SN)_2(NO)_2]$ (**4-PPh$_4$**) (dashed line) in 0.1 M $[TBA][PF_6]$ with a glassy carbon working electrode at a scan rate of 1 V s^{-1}.

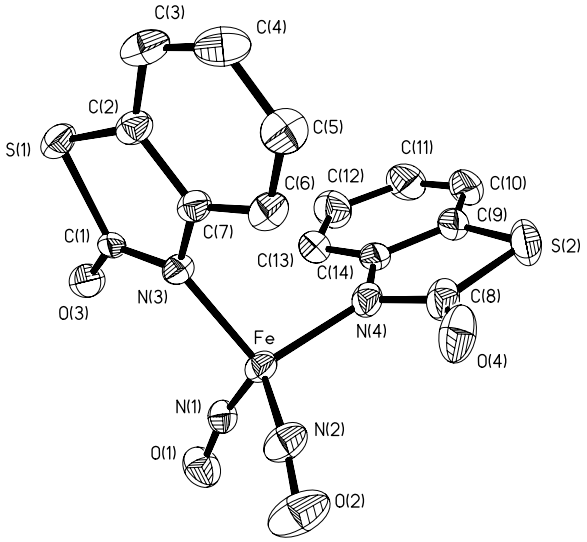

Figure S2. ORTEP diagram of the anion of $[PPh_4][Fe(OC_7H_4SN)_2(NO)_2]$ (**4-PPh$_4$**) showing 50% thermal ellipsoids for all non-hydrogen atoms. Selected bond distances (Å) and angles (deg): Fe−N(1), 1.685(2); Fe−N(2), 1.688(2); Fe−N(3), 1.992(2); Fe−N(4), 1.994(2); N(1)−O(1), 1.178(3); N(2)−O(2), 1.172(3); N(1)−Fe−N(2), 111.23(11); N(3)−Fe−N(4), 101.84(9); N(1)−Fe−N(3), 111.04(10); N(2)−Fe−N(3), 112.12(10); Fe−N(1)−O(1), 162.8(2); Fe−N(2)−O(2), 164.3(2).

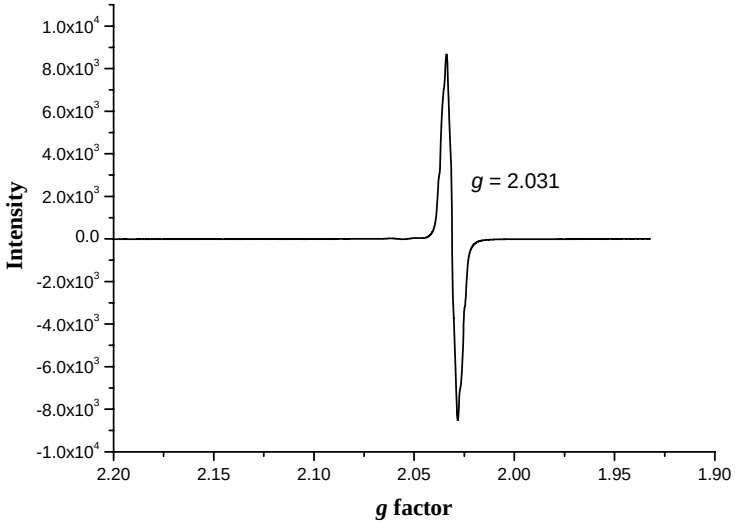

Figure S3. X-band EPR spectrum of $[PPh_4][Fe(OC_7H_4SN)_2(NO)_2]$ (**4-PPh$_4$**) in THF at 298 K.

Tables

Table S1. Crystal data and structure refinement for complex **1-PPh$_4$**.

Empirical formula	C62 H48 Fe N4 O2 P2 S4	
Formula weight	1127.07	
Temperature	200(2) K	
Wavelength	0.71073 Å	
Crystal system	Monoclinic	
Space group	P 21/n	
Unit cell dimensions	a = 10.6617(2) Å	α= 90°.
	b = 36.6398(6) Å	β= 96.0940(10)°.
	c = 14.0069(3) Å	γ = 90°.
Volume	5440.77(18) Å^3	
Z	4	
Density (calculated)	1.376 Mg/m^3	
Absorption coefficient	0.538 mm^{-1}	
F(000)	2336	
Crystal size	0.38 x 0.25 x 0.07 mm^3	
Theta range for data collection	2.22 to 25.06°.	
Index ranges	-12<=h<=12, -38<=k<=43, -16<=l<=12	
Reflections collected	17171	
Independent reflections	9448 [R(int) = 0.0631]	
Completeness to theta = 24.86°	96.6 %	
Absorption correction	Semi-empirical from equivalents	
Max. and min. transmission	0.9648 and 0.8397	
Refinement method	Full-matrix least-squares on F^2	
Data / restraints / parameters	9448 / 0 / 676	
Goodness-of-fit on F^2	1.034	
Final R indices [I>2sigma(I)]	R1 = 0.0522, wR2 = 0.1127	
R indices (all data)	R1 = 0.0974, wR2 = 0.1354	
Largest diff. peak and hole	0.280 and -0.381 e.Å^{-3}	

Table S2. Crystal data and structure refinement for complex **2-PPh$_4$**.

Empirical formula	C62 H48 Fe N4 O4 P2 S2	
Formula weight	1094.95	
Temperature	293(2) K	
Wavelength	0.71073 Å	
Crystal system	Monoclinic	
Space group	C 2/c	
Unit cell dimensions	a = 23.4730(5) Å	α= 90°.
	b = 13.4520(3) Å	β= 119.0330(10)°.
	c = 19.3090(5) Å	γ = 90°.
Volume	5330.8(2) Å^3	
Z	4	
Density (calculated)	1.364 Mg/m^3	
Absorption coefficient	0.475 mm^{-1}	
F(000)	2272	
Crystal size	0.58 x 0.4 x 0.32 mm^3	
Theta range for data collection	2.26 to 25.04°.	
Index ranges	-23<=h<=26, -15<=k<=15, -13<=l<=22	
Reflections collected	12513	
Independent reflections	4446 [R(int) = 0.0486]	
Completeness to theta = 25.04°	94.4 %	
Absorption correction	Semi-empirical from equivalents	
Max. and min. transmission	0.7552 and 0.596	
Refinement method	Full-matrix least-squares on F^2	
Data / restraints / parameters	4446 / 0 / 339	
Goodness-of-fit on F^2	1.011	
Final R indices [I>2sigma(I)]	R1 = 0.0463, wR2 = 0.1232	
R indices (all data)	R1 = 0.0608, wR2 = 0.1344	
Largest diff. peak and hole	0.681 and -0.558 e.Å^{-3}	

Table S3. Crystal data and structure refinement for complex **4-PPh$_4$**.

Empirical formula	C38 H28 Fe N4 O4 P S2	
Formula weight	755.58	
Temperature	150(2) K	
Wavelength	0.71073 Å	
Crystal system	Orthorhombic	
Space group	Pbca	
Unit cell dimensions	a = 15.5535(8) Å	α= 90°.
	b = 16.8415(8) Å	β= 90°.
	c = 26.5880(12) Å	γ = 90°.
Volume	6964.6(6) Å^3	
Z	8	
Density (calculated)	1.441 Mg/m^3	
Absorption coefficient	0.646 mm^{-1}	
F(000)	3112	
Crystal size	0.40 x 0.25 x 0.25 mm^3	
Theta range for data collection	1.94 to 27.50°.	
Index ranges	-20<=h<=20, -21<=k<=16, -34<=l<=18	
Reflections collected	34619	
Independent reflections	7993 [R(int) = 0.0674]	
Completeness to theta = 27.50°	100.0 %	
Absorption correction	Semi-empirical from equivalents	
Max. and min. transmission	0.8551 and 0.7821	
Refinement method	Full-matrix least-squares on F^2	
Data / restraints / parameters	7993 / 0 / 451	
Goodness-of-fit on F^2	1.042	
Final R indices [I>2sigma(I)]	R1 = 0.0506, wR2 = 0.1063	
R indices (all data)	R1 = 0.0769, wR2 = 0.1172	
Largest diff. peak and hole	0.632 and -0.375 e.Å^{-3}	

國科會補助計畫衍生研發成果推廣資料表

日期:2011/08/15

國科會補助計畫	計畫名稱: 雙亞硝醯基鐵化合物之合成，反應性研究及其電子結構與作為一氧化氮傳遞劑效率探討
	計畫主持人: 陳建宏
	計畫編號: 99-2119-M-040-001- 學門領域: 無機化學

無研發成果推廣資料

99 年度專題研究計畫研究成果彙整表

計畫主持人：陳建宏	計畫編號：99-2119-M-040-001-
計畫名稱：雙亞硝醯基鐵化合物之合成，反應性研究及其電子結構與作為一氧化氮傳遞劑效率探討	

成果項目			量化			單位	備註（質化說明：如數個計畫共同成果、成果列為該期刊之封面故事...等）
			實際已達成數（被接受或已發表）	預期總達成數(含實際已達成數)	本計畫實際貢獻百分比		
國內	論文著作	期刊論文	0	0	100%	篇	
		研究報告/技術報告	0	0	100%		
		研討會論文	0	0	100%		
		專書	0	0	100%		
	專利	申請中件數	0	0	100%	件	
		已獲得件數	0	0	100%		
	技術移轉	件數	0	0	100%	件	
		權利金	0	0	100%	千元	
	參與計畫人力（本國籍）	碩士生	2	2	100%	人次	
		博士生	0	0	100%		
		博士後研究員	0	0	100%		
		專任助理	0	0	100%		
國外	論文著作	期刊論文	1	1	100%	篇	
		研究報告/技術報告	0	0	100%		
		研討會論文	0	0	100%		
		專書	0	0	100%	章/本	
	專利	申請中件數	0	0	100%	件	
		已獲得件數	0	0	100%		
	技術移轉	件數	0	0	100%	件	
		權利金	0	0	100%	千元	
	參與計畫人力（外國籍）	碩士生	0	0	100%	人次	
		博士生	0	0	100%		
		博士後研究員	0	0	100%		
		專任助理	0	0	100%		

其他成果 (無法以量化表達之成果如辦理學術活動、獲得獎項、重要國際合作、研究成果國際影響力及其他協助產業技術發展之具體效益事項等，請以文字敘述填列。)	無

	成果項目	量化	名稱或內容性質簡述
科教處計畫加填項目	測驗工具(含質性與量性)	0	
	課程/模組	0	
	電腦及網路系統或工具	0	
	教材	0	
	舉辦之活動/競賽	0	
	研討會/工作坊	0	
	電子報、網站	0	
	計畫成果推廣之參與（閱聽）人數	0	

國科會補助專題研究計畫成果報告自評表

請就研究內容與原計畫相符程度、達成預期目標情況、研究成果之學術或應用價值（簡要敘述成果所代表之意義、價值、影響或進一步發展之可能性）、是否適合在學術期刊發表或申請專利、主要發現或其他有關價值等，作一綜合評估。

1. 請就研究內容與原計畫相符程度、達成預期目標情況作一綜合評估

■達成目標

□未達成目標（請說明，以 100 字為限）

□實驗失敗

□因故實驗中斷

□其他原因

說明：

2. 研究成果在學術期刊發表或申請專利等情形：

論文：■已發表 □未發表之文稿 □撰寫中 □無

專利：□已獲得 □申請中 ■無

技轉：□已技轉 □洽談中 ■無

其他：(以 100 字為限)

3. 請依學術成就、技術創新、社會影響等方面，評估研究成果之學術或應用價值（簡要敘述成果所代表之意義、價值、影響或進一步發展之可能性）(以 500 字為限)

經由 Fe(TMEDA)(NO)2 與分別與兩當量[SC7H4SN]讣 and [OC7H4SN]讣反應可以得到第一個含[硫基,硫基]及[胺基,胺基]的負二價雙亞硝醯基鐵化合物([Fe(SC7H4SN)2(NO)2]2 讣 (1) [Fe(OC7H4SN)2(NO)2]2 讣 (2))。負二價雙亞硝醯基鐵化合物(DNICs 1/2)與負一價雙亞硝醯基鐵化合物([Fe(SC7H4SN)2(NO)2]讣 (3) [Fe(OC7H4SN)2(NO)2]讣 (4) (DNICs 3/4))之間的相互轉換也成功的被證實。利用這四個化合物的反應比較，我們發現[SC7H4SN]讣對雙亞硝醯基鐵化合物中{Fe(NO)2}10 的單元親和力較好,而[OC7H4SN]讣 則對雙亞硝醯基鐵化合物中{Fe(NO)2}9 的單元親和力較好。另外我們也發現要得到相對穩定的雙亞硝醯基鐵化合物，除了以交換配位子的方式來進行之外，直接進行分子間的電子轉移亦可能是另外的一個途徑。